ONLINE SUPPLEMENT

SUPPLEMENTAL METHODS:

Animal protocols: Animal experiments were conducted in accordance with the National Institutes of Health Guide for the Care and Use of Laboratory Animals and were approved by the Baylor College of Medicine and Albert Einstein College of Medicine Institutional Review Boards. Male and female, 2-4 month-old wildtype (WT) and tTG knockout (KO) [1] mice in a C57BL/6J background from our colony were genotyped using established protocols. Animals were anesthetized with inhaled isoflurane. Aortic banding was achieved by creating a constriction between the right innominate and left carotid arteries, as previously described [2]. The degree of pressure overload was assessed by measuring right-to-left carotid artery flow velocity ratio after constricting the transverse aorta. At the end of the experiment, the heart was excised, fixed in zinc-formalin, and embedded in paraffin for histological studies, or frozen for RNA/protein isolation. Animals used for histology underwent 3, 7, and 28 days of banding (n=8 per group). Additional groups of mice were used for RNA and protein extraction after 7 (n=8 per group) or 28 days (n=8 per group) of banding, and for isolation and flow cytometric analysis of interstitial cells (n=3 per group). As a control, a "sham" operation without aortic constriction was performed on age-matched mice (WT, n=31; KO n=39).

Echocardiography: Short axis M-mode echocardiography was performed prior to instrumentation and before the end of each experiment (7 or 28 days of TAC, n=20 per group) using the Vevo 2100 system (VisualSonics, Toronto ON), as previously described [3]. The following parameters were measured as indicators of function and remodeling: left ventricular end-diastolic diameter (LVEDD), left ventricular end-systolic diameter (LVESD), left ventricular end-diastolic volume (LVEDV), left ventricular end-systolic volume (LVESV), ejection fraction, and end-diastolic left ventricular anterior wall thickness (LVAWTd).

Doppler echocardiography and tissue Doppler imaging: 3-4 month-old WT and tTG KO mice underwent Doppler echocardiography and tissue Doppler imaging at baseline to assess diastolic function using the Vevo 2100 system (VisualSonics). Transmitral LV inflow velocities were measured from apical 4-chamber view by pulsed-wave Doppler. Peak early E (E-wave) and late

A (A-wave) filling velocities and E/A ratio were measured according to the guidelines of the American Society of Echocardiography[4]. Tissue Doppler imaging of the mitral annulus was obtained from the apical 4-chamber view. A 1.0-mm sample volume was placed sequentially at the medial mitral annulus. Analysis was performed for systolic velocity and for the early (E') and late diastolic velocity (A'). The off-line analysis was performed by a sonographer blinded to study groups.

Pressure:volume loop analysis: Left ventricular pressure-volume analysis was performed using progressive isovolumic Langendorff retrograde perfusion of isolated murine hearts, as previously described [5,6]. LVDP was calculated as the difference between peak-systolic pressure and LV end-diastolic pressure (LVEDP). Three independent runs for each animal were collected and averaged for the purpose of calculation. A final pressure-volume exponential relationship was obtained. The data for LVEDP were plotted as a function of increasing balloon volumes, and to a best-fit exponential curve ($P=b \cdot \exp(KV)$), where V is volume, and P is LV pressure generated for each mouse. The volumes at a given pressure were averaged for animals in each group. The chamber stiffness constant (K) was determined by fitting the end-diastolic pressure-volume curves from individual hearts to an exponential function [7,8].

Immunohistochemistry, dual fluorescence and quantitative histology: All tissue sections were cut at 5 μm and stained either immunohistochemically or processed for immunofluroescence. Myofibroblasts were identified by staining with an antibody to α- smooth muscle actin (α-SMA) (Clone 1A4, Sigma) (1:100) as spindle-shaped cells located outside the vascular media. Macrophages were labeled using a rat anti-mouse Mac-2 antibody (Cedarlane, Burlington NC) (1:200). Ten random fields from two different sections from each animal were used for quantitation. Quantitative assessment of myofibroblast and macrophage density was performed by counting the number of cells/myocardial area using Image Pro Plus software. Cell density was expressed as cells/mm². Cardiomyocytes were outlined using wheat germ agglutinin (WGA) histochemistry, as previously described using an Alexa Fluor® 594 Conjugate (Life Technologies) (dilution 1:100) [9]. Cardiomyocyte size was quantified using Axiovision LE 4.8 software (Zeiss). Cardiomyocyte area was expressed in μm^2. Collagen fibers were labeled using picrosirius red staining. Collagen content was measured using Image Pro Plus software. Collagen content was expressed as the fraction of the picrosirius-red stained area in the fields used for analysis. Fifteen fields from three non-adjacent stained sections per mouse base, mid-

myocardium and apex of each heart were used for analysis of collagen content and cardiomyocyte size. For immunofluorescence experiments: tTG was immunolocalized using a rabbit polyclonal anti-transglutaminase II antibody (Ab-4, Lab Vision, ThermoFisher Scientific) (1:500). A rat anti-mouse Mac-2 antibody (Cedarlane, Burlington NC) (1:200) and an anti-α-SMA antibody (Clone 1A4, Sigma) (1:100) were used for macrophage and myofibroblast staining respectively. A rabbit polyclonal antibody to pan-cadherin (Abcam) (1:500) was used to label the cytoplasmic membrane in collagen pads. For studies examining the cellular localization of tTG, dual immunofluorescence combining tTG/α-SMA, tTG/Mac-2, tTG/WGA, and tTG/pan-cadherin staining was performed. A mouse monoclonal antibody against TIMP1 (F31 P2 A5, ThermoFisher Scientific)[10] at a concentration of 2 μg/ml was used to stain TIMP1 protein in fibroblasts embedded in collagen pads. A rabbit polyclonal p-Smad2 (Ser 465/467) antibody (3101S, Cell Signaling Technology) (1:50) was used to stain phospho-Smad2 in collagen pad fibroblasts.

Polarized light microscopy for assessment of collagen content: Polarized light microscopy was used to assess collagen deposition, as previously described by Whittaker et al. [11]. Briefly, paraffin sections (5 μ thick) were stained using picrosirius red. Circularly polarized images were obtained using Axio Imager M2 for polarized light microscopy (Zeiss). When the collagen fibers are stained with picrosirius red and viewed with polarized light, depending on the thickness of the collagen fibers, the hues range from green to yellow to orange to red. The respective proportions of different hues were assessed using Image J software. The 8-bit hue images contain 256 colors and we distinguished different colors based on visible hues. We used the following hue definitions; red 2-9 and 230-256, orange 10-38, yellow 39-51, green 52-128. The number of pixels within each hue range was expressed as a percentage of the total number of collagen pixels, which in turn was expressed as a percentage of the total number of pixels in the image. At least 12 different fields were obtained and analyzed per heart sample.

Assessment of apoptosis using TUNEL staining and WGA lectin fluorescence: Identification of apoptotic cardiomyocytes and interstitial cells in pressure-overloaded hearts was performed using fluorescent *In situ* Cell Death Detection Kit (Roche) and WGA staining (to visualize cardiomyocytes by labeling cell membranes and the surrounding extracellular matrix) as previously described [12].

RNA extraction and qPCR: Isolated total RNA from mouse hearts was reverse transcribed to cDNA using the iScript™ cDNA synthesis kit (Bio-Rad) following the manufacturer's guidelines. Quantitative PCR was performed using the SsoFast™ EvaGreen® Supermix (Bio-Rad) method on the CFX384™ Real-Time PCR Detection System (Bio-Rad). Primers were synthesized at the Baylor College of Medicine Child Health Research Center core facility and by Integrated DNA Technologies. The following sets of primers were used in the study: tTG forward: TGCTTCTCACCTATGACT, reverse: ATATTTAAGGCTCGTTCTGT; transglutaminase 1 (TG1) forward: TGTTATTCAAGTGGATGT, reverse: TCGATATGCCATAGGTAT; TG3 forward: GGCAGTTGGTAGACATAT, reverse: ATGAGAATGGATTGTTGTG; TG4 forward: ACAGGCAAACATTTCAAA, reverse: TTCTATATCTGGGCTCTG; TG5 forward: AGGTCTCTCTGAAGTTTG, reverse: TTGAGATCCTTGAACTGA; TG6 forward: ACCAGAGTAGACACAACAA, reverse: TATCCAAGAGGCACTGAG; TG7 forward: GGAGTACAGAGGATGATG, reverse: AGGTAATGGAATTTGTTTGA; coagulation factor XIII, A1 subunit (FXIIIa1) forward: GCTATGGAGATTCTAATGC, reverse: GGTGTGCCTATGAAATAC; TIMP-1 forward GCCTGAACACTGTCTACTT reverse TTGCTGCTGTCTGATAGTT; MMP-2 forward TCCGCTGCATCCAGACTT, reverse GGTCCTGGCAATCCCTTTGTATA; MMP-3 forward ATTTGGGTTTCTCTACTT, reverse GAAGAACTATAAGCATCAG; MMP-9 forward TCTTACATTGGAGAACAC , reverse GAAGGAAGAACCAACATT; Lysyl oxidase forward: CTTTCCCAGACCTTCGTGCG, reverse: GCGAGAAACCAGCTTGGAAC; Lysyl oxidase homolog 1, forward: AGAGAAGACACATGAATT, reverse: GAGTTCTAGGATACCATAT; Lysyl oxidase homolog 2, forward: AATTATAGCCACGACTTA, reverse: TGACTTTCTCTTCCTATC; Lysyl oxidase homolog 3, forward: AACTTCACTTCTGTCATC, reverse: TTCCACTTCTATGTCTCA; Lysyl oxidase homolog 4, forward: GGACTTCTTACTACTAATAC, reverse: TAACTCTCAGGATAACTC.

Hydroxyproline biochemical assay: To assess crosslinking of collagen in pressure overloaded hearts we adopted a method described by Mukherjee et al [13]. In this method, PBS and sodium dodecyl sulfate (SDS) are used to remove the bulk of non-collagenous proteins and freshly deposited collagen, leaving insoluble residue of crosslinked collagen. Incubation with cyanogen bromide (CNBr) allows determining the degree of collagen cross-linking based on solubility to

CNBr [6]. Total and insoluble collagen was expressed as μg of collagen/mg of dry tissue. The index of collagen crosslinking was defined as ratio of insoluble collagen to total collagen.

Zymography: MMP activity in the pressure overloaded myocardium was examined by gelatin zymography as previously described [6].

Flow cytometry: Suspensions of interstitial cells were prepared from WT and tTG KO hearts after 7 days of TAC. Briefly, hearts were rapidly excised and placed in ice-cold Krebs-Henseleit (KH) buffer containing (in g/L) 2 glucose, 0.141 $MgSO_4$, 0.16 NaH_2PO_4, 0.35 KCl, 6.9 NaCl, 2.1 $NaHCO_3$, 0.373 $CaCl_2$, 1 NaN_3 at pH 7.4. Subsequently, the aorta was cannulated with a 22-gauge tubing adaptor and flushed with ice-cold KH buffer to remove residual cells in the coronary vasculature. Hearts were weighted and minced with fine scissors and placed into a cocktail of 0.25 mg/ml Liberase Blendzyme 3 (Roche Applied Science), 20 U/ml DNase I (Sigma Aldrich), 10 mmol/L HEPES (Invitrogen), 0.1% Sodium Azide in HBSS with Ca^{2+} and Mg^{2+} (Invitrogen) and shaken at 37°C for 40 minutes. Cells were then passed through a 40-μm nylon mesh (BD Falcon), centrifuged (10 minutes, 500*g*, 4°C), and resuspended in 0.1% sodium azide solution in HBSS without Ca^{2+} and Mg^{2+}. Cell yield from hearts was calculated with hematocytometer. 5×10^5 to 10^6 cells were incubated with either anti-FcγIII/II (clone 2.4G2) antibody (BD Pharmingen) for 5 minutes and labeled at 4°C for 30 minutes with either FITC-labeled anti-CD45 (clone 30-F11) or FITC anti-CD31. For intracellular staining, cells were fixed, permeabilized for 45 minutes at 4°C with fixation/permabilization kit (eBioscience) and stained with FITC-conjugated anti-α-SMA (Sigma, Clone 1A4) and purified rabbit anticollagen I (Rockland Inc.) antibodies. Cell permeable DRAQ5 dye (Alexis Biochemicals) was used to define the gate for nucleated cells. Finally, cells were washed twice, resuspended in staining buffer, and immediately analyzed with a Cell Lab Quanta SC flow cytometer (Beckman Coulter). Data analysis was performed using FlowJo (Tree Star, Inc.). Cell densities were expressed per mg of heart tissue.

Cardiac fibroblast isolation and stimulation: Cardiac fibroblasts were isolated from WT, Smad3 KO and tTG KO animals as previously described [12,14]. Mice were euthanized using 2% inhaled isoflurane followed by cervical dislocation. TGF-β stimulation experiments were performed using recombinant TGF-β1 (R&D Systems) for 4h. tTG mRNA expression was compared between WT and Smad3 -/- cells using qPCR. Fibroblasts isolated from WT and tTG

KO hearts were stimulated with TGF-β1 for 5-30 min and protein was extracted for assessment of Smad phosphorylation.

Western blotting: Protein was isolated from stimulated cells. Western blotting was performed using the following antibodies: rabbit anti-mouse p-Smad2 (ser465/467) (Cell Signaling) and rabbit anti-Smad2 (Cell Signaling).

Studies on cardiac fibroblasts populating collagen pads: Cardiac fibroblasts isolated from WT and tTG KO animals were cultured to passage 2 and serum-starved overnight (16 hrs). Collagen matrix was prepared on ice by diluting a stock solution of rat 3.0 mg/ml collagen I (GIBCO Invitrogen Corporation, Carlsbad, CA) with 2X MEM and distilled water for a final concentration of 1 mg/ml collagen. Cell suspensions in 2X MEM were mixed with collagen solution to achieve the final $3*10^5$ cells/ml concentration. Subsequently, 500 µl of this suspension was aliquoted to a 24-well culture plate (BD Falcon, San Jose, CA) and allowed to polymerize at 37ºC for 30 min. Following polymerization, pads were released from wells, transferred to 6-well culture plate (BD Falcon, San Jose, CA) and cultured in 0% FCS DMEM/F12 for 24 h. After incubation, the pads were used for RNA extraction and subsequent analyses. For growth factor stimulation experiments, the collagen pads were suspended in either serum free DMEM/F12 or with 10% fetal bovine serum or TGF-β or basic Fibroblast Growth Factor (bFGF) (50 ng/ml) for 24 hours. For experiments examining the effects of tTG on fibroblast phenotype, enzymatically active recombinant mouse tTG produced in E.coli (T040, Zedira GmbH) was incorporated into collagen pads at a concentration of 50µg/ml. To differentiate between enzymatic and non-enzymatic effects of tTG, fibroblasts were cultured in collagen pads in the presence or absence of a recombinant human tissue transglutaminase (His_6-rhTG2-Cys277Ser) (T018, Zedira GmbH), which due to Cys277Ser mutation has no transglutaminase activity (concentration: 50 µg/ml). In order to examine the role of interactions involving β1 integrins, tTG-stimulated fibroblasts were pretreated with the anti-β1 integrin antibody HMβ1-1 (25 µg/ml, Millipore).

Macrophage isolation and stimulation: In order to examine the effects of cytokines on expression of tTG by macrophages, CD11b+ macrophages were isolated from the mouse spleen using immunomagnetic sorting with Miltenyi microbeads (Miltenyi Biotech, Bergish Gladbach, Germany) as previously described [14]. Mice were euthanized using 2% inhaled isoflurane followed by cervical dislocation. The cells were stimulated with Interleukin (IL)-1β and TGF-β1

(from R&D Systems) for 4h. At the end of the experiment, cells were harvested for RNA extraction. In order to examine whether the effects of TGF-β1 were mediated through Smad3, tTG expression was compared between macrophages harvested from WT and Smad3 KO mice (from our own colony)[12]. In order to study the effects of tTG loss on phenotypic modulation of macrophages following pressure overload, we compared gene expression between CD11b+ myeloid cells sorted from pressure-overloaded WT and tTG KO hearts after 7 days of TAC.

Assessment of plasma glucose levels: 4-6 month-old WT and tTG knockout mice both male and female, with body weights ranging from 15 to 25 gm; were used for blood glucose assessment. After an overnight fast of 16 h, blood was drawn from the tail vein and plasma glucose levels were determined using an automatic glucometer (Nova Max Blood Glucose Monitoring System, Nova Diabetes Care, Inc., MA). Glucose measurements were repeated twice for each mouse and averaged.

Measurement of systemic blood pressure: Blood pressure in mice was measured non-invasively using the CODA monitor from Kent Scientific (Torrington, CT). The monitor measures tail blood pressure by determining the tail blood volume, using a volume pressure recording (VPR) tail cuff and an occlusion tail cuff. The tails of the mice were inserted into the tail cuffs, with the occlusion cuff (size extra-small) being positioned at the base of the tail and the VPR cuff being positioned 2mm behind the occlusion cuff. Blood pressure was measured through 15 cycles for each mouse. The first five cycles were acclimation cycles and were not included into the final data, while the remaining ten cycles were used to generate an average systolic, diastolic, and mean blood pressure for each mouse. Twelve C57 mice in total were used to measure blood pressure: six WT (3 males and 3 females) and six tTG knockouts (3 males and 3 females).

Statistical analysis: Comparisons between more than 2 groups were performed using one-way ANOVA followed by t-test corrected for multiple comparisons (Sidak's test). For non-Gaussian distributions, non-parametric ANOVA was used (Kruskal-Wallis). Comparisons between 2 groups were performed using unpaired t-test, or the Mann-Whitney test (for non-Gaussian distributions). Mortality was compared using the log rank test. Data were expressed as mean±SEM. Statistical significance was set at 0.05.

SUPPLEMENTAL FIGURES:

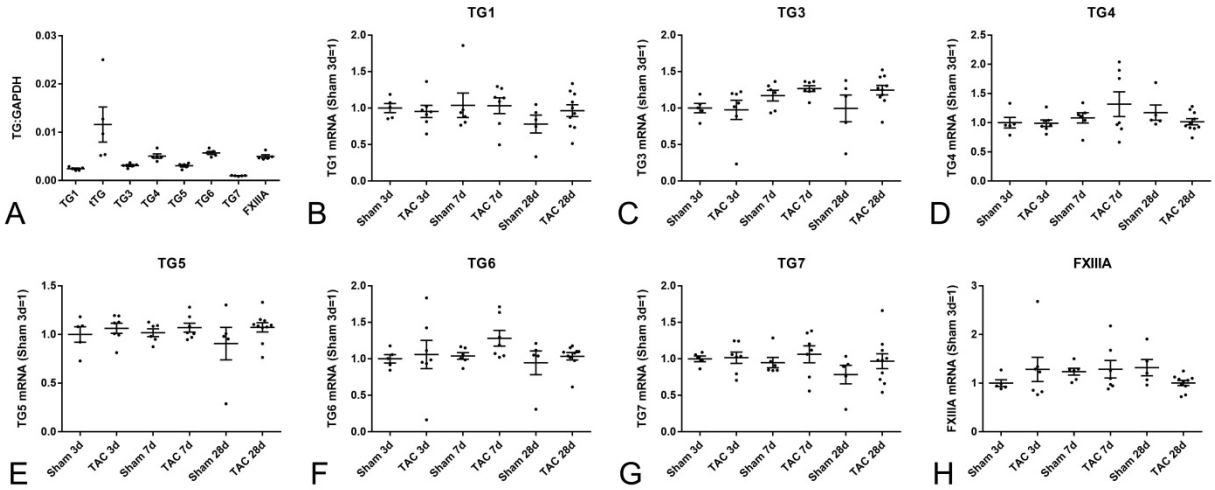

Supplemental figure 1: qPCR analysis shows expression of transglutaminases in the pressure-overloaded myocardium. A. Comparison of transglutaminase expression in sham hearts shows that in the absence of injury, tTG is the most abundantly expressed transglutaminase in the myocardium. TG4, TG6 and FXIIIA also exhibit significant myocardial expression. B-H. In comparison to sham hearts, expression of TG1 (B), TG3 (C), TG4 (D), TG5 (E), TG6 (F), TG7 (G) and FXIIIA (H) was not significantly increased following pressure overload (n=5-12/group, p=NS, Kruskal-Wallis).

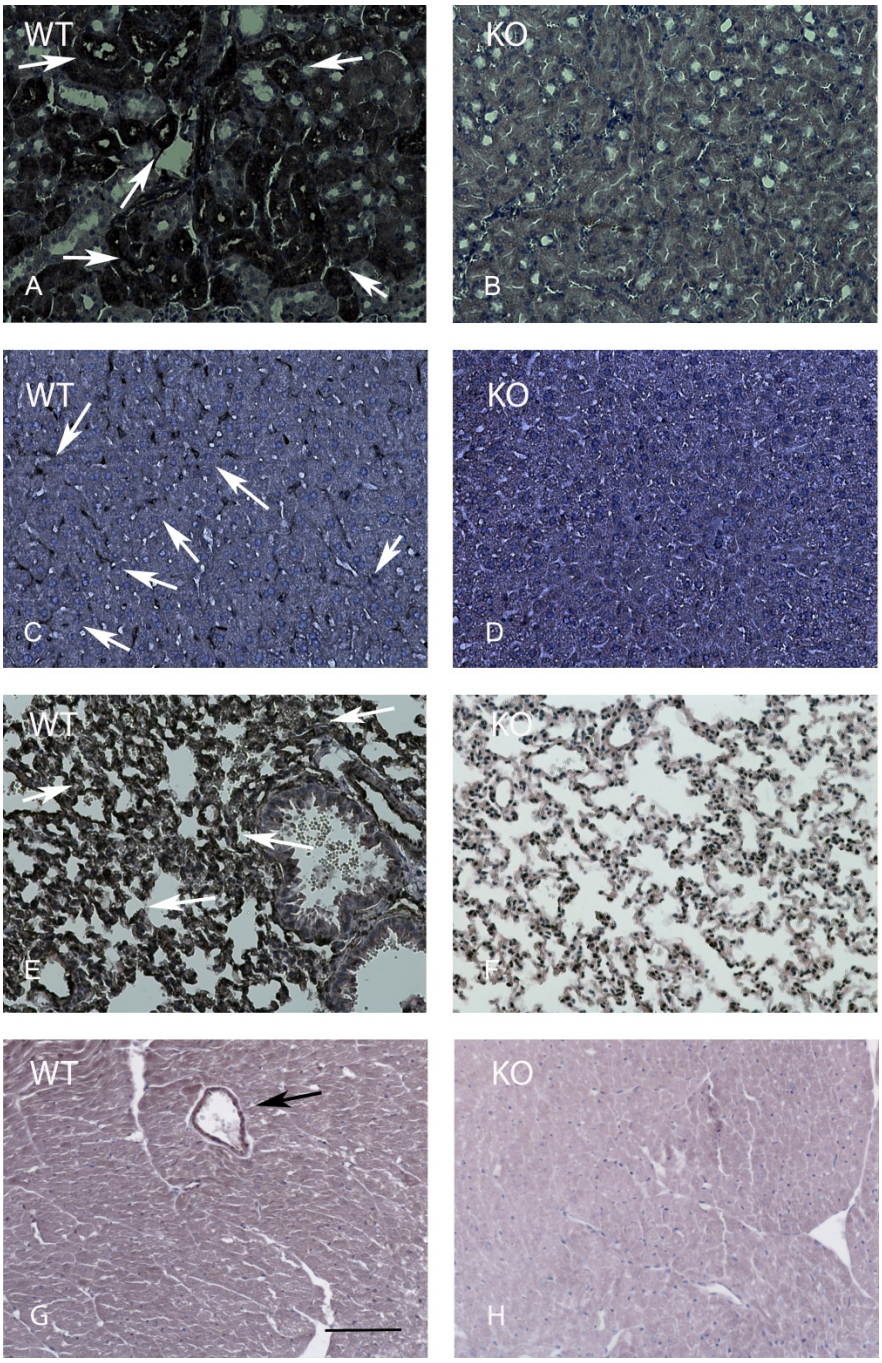

Supplemental figure 2: Documentation of the specificity of the rabbit polyclonal anti-tTG antibody using sections from mouse kidney (A, B), liver (C, D) and lung (E, F). In WT mouse kidney (A), intense tTG immunoreactivity was predominantly localized in tubular epithelial cells (arrows). In KO kidney, tTG immunoreactivity was low. In WT liver (C), but not in KO liver (D) interstitial cells with morphological characteristics of hepatic macrophages expressed high levels of tTG (arrows). In WT mouse lung (E), but not in KO lung (F) tTG immunoreactivity was predominantly localized in macrophages (arrows). tTG expression in macrophages is consistent with recently reported observations in mouse and human tissues [15]. In WT mouse heart (G), tTG was expressed in cardiomyocytes and vascular cells (arrows). In contrast, very low level tTG immunoreactivity was noted in tTG KO myocardium (scalebar=50μm).

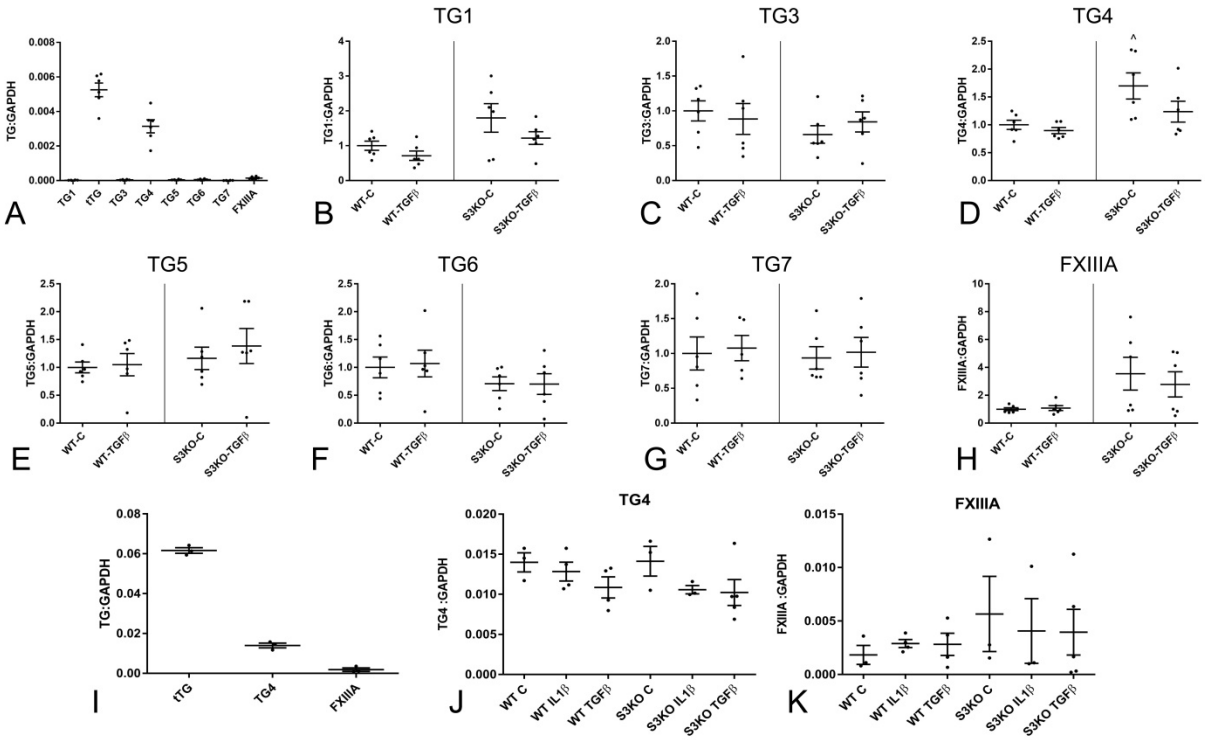

Supplemental figure 3: Expression of transglutaminases (TG) in stimulated cardiac fibroblasts (n=6/group) and splenic macrophages (n=3-5/group). A. tTG was the highest-expressed TG in unstimulated cardiac fibroblasts. Cardiac fibroblasts also expressed TG4, but exhibited very low levels of expression of TG1, TG3, TG5, TG6, TG7 and FXIII. TGF-β stimulation did not significantly affect expression of TG1 (B), TG3 (C), TG4 (D), TG5 (E), TG6 (F), TG7 (G) and FXIII (H). Smad3 KO fibroblasts exhibited higher levels of TG4 expression than WT cells (^$p<0.05$, n=5-6, Kruskal-Wallis). I. tTG was the highest-expressed TG in unstimulated splenic macrophages. TG4 and FXIII were also expressed; in contrast, other TGs could not be detected. TGF-β stimulation did not significantly modulate TG4 (J) and FXIII (K) expression in splenic macrophages. Smad3 KO splenic macrophages and WT cells exhibited comparable TG4 and FXIII expression in the presence or absence of TGF-β1 (J-K).

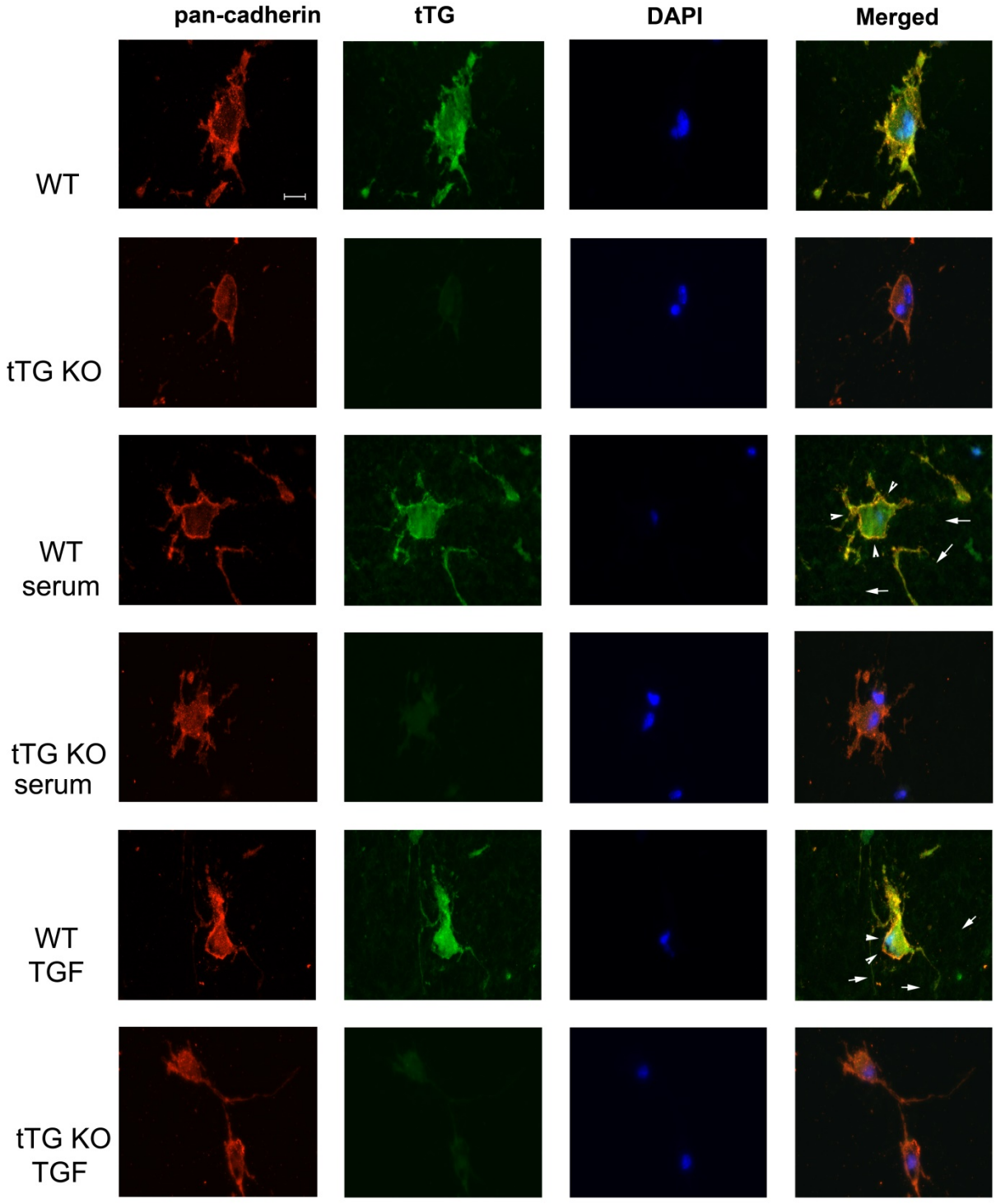

Supplemental figure 4: Stimulated cardiac fibroblasts release tTG into the extracellular matrix. Dual immunofluorescence for pan-cadherin (red) to label the cytoplasmic membrane (arrowheads) and tTG (green) shows that upon stimulation with serum or TGF-β1, cardiac fibroblasts show increased tTG fluorescence and release tTG into the surrounding extracellular

matrix (arrows). tTG KO cells were used as negative controls, showing negligible tTG immunofluorescence (scalebar=20μm).

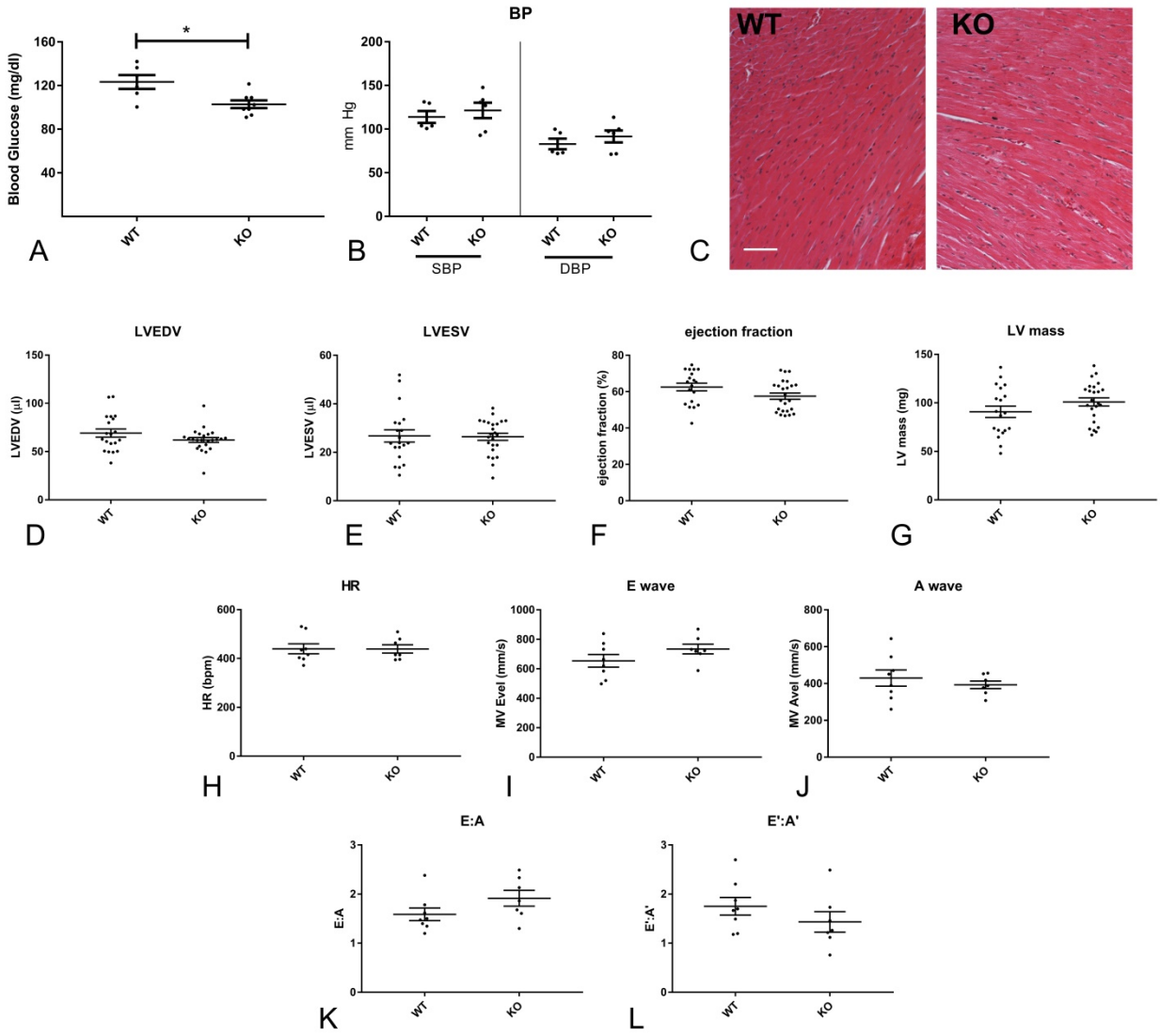

Supplemental figure 5: Effects of global tTG loss on baseline phenotype and cardiac function. A. Adult tTG KO mice had a modest, but statistically significant reduction in fasting blood glucose levels (*$p<0.05$ vs. WT, n=6-8/group, unpaired t-test). B. tTG loss did not significantly affect systolic and diastolic blood pressure (SBP, DBP respectively – n=5-6/group). C. Morphological analysis of the myocardium using H&E staining showed no significant effects of global tTG loss on cardiac morphology (scalebar=60µm). D-G. Echocardiographic analysis showed that in the absence of injury, WT and tTG KO mice have comparable left ventricular end-diastolic volume (LVEDV, D), left ventricular end-systolic volume (LVESV, E), ejection fraction (F) and LV mass (G) (p=NS, n=20-24/group, unpaired t-test). H-L. Mitral inflow Doppler and tissue Doppler imaging were used to assess diastolic function. tTG KO and WT animals had no significant differences in heart rate (HR, H), E wave velocity (I), A wave velocity (J), E:A (K) and E':A' (L) ratio suggesting comparable diastolic function (p=NS, n=7-8/group, unpaired t-test).

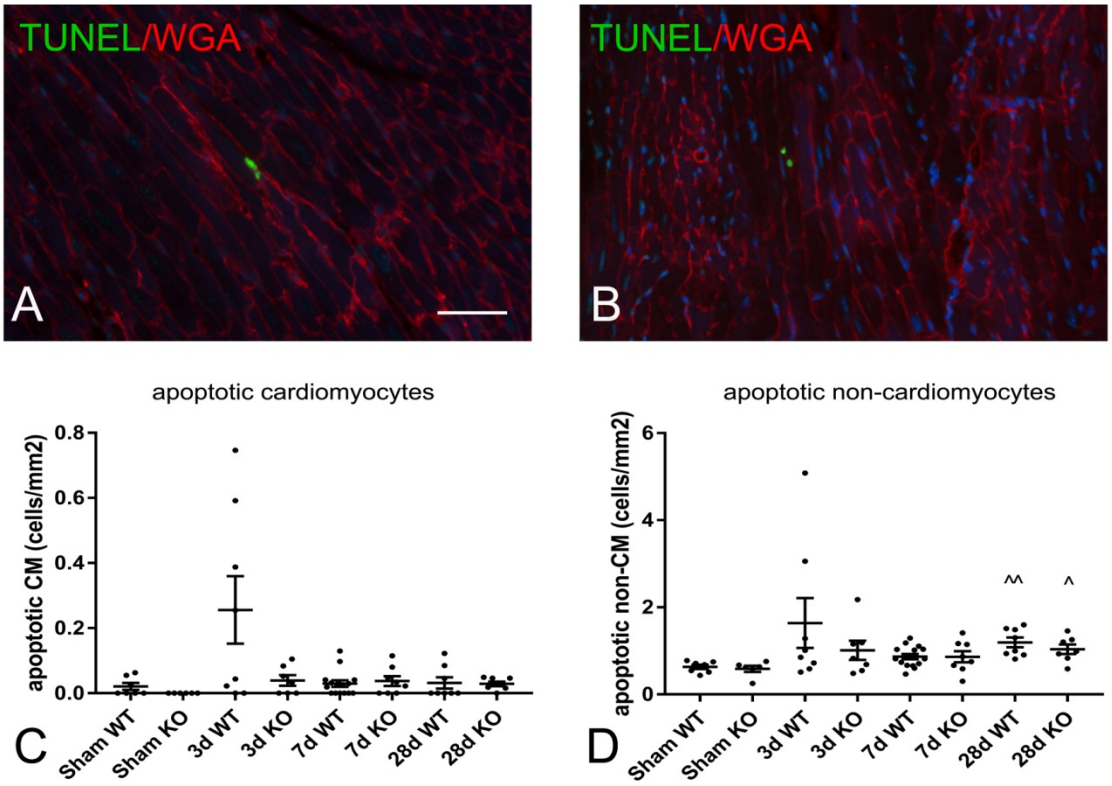

Supplemental figure 6: tTG loss does not affect cardiomyocyte apoptosis in the remodeling pressure-overloaded myocardium. A-B. Representative images show apoptotic cells, labeled in the pressure overloaded WT (A) and tTG KO (B) myocardium after 7 days of TAC, using TUNEL staining (green). Cardiomyocytes were identified using WGA lectin staining (red). Apoptotic cells were very rare in the pressure-overloaded myocardium at all timepoints examined. C-D: Quantitative analysis showed no significant differences between WT and tTG KO animals in density of apoptotic cardiomyocytes (C) and non-cardiomyocytes (D) (*$p<0.05$ vs. sham, n=6-16/group, Kruskal-Wallis). Scalebar=60μm.

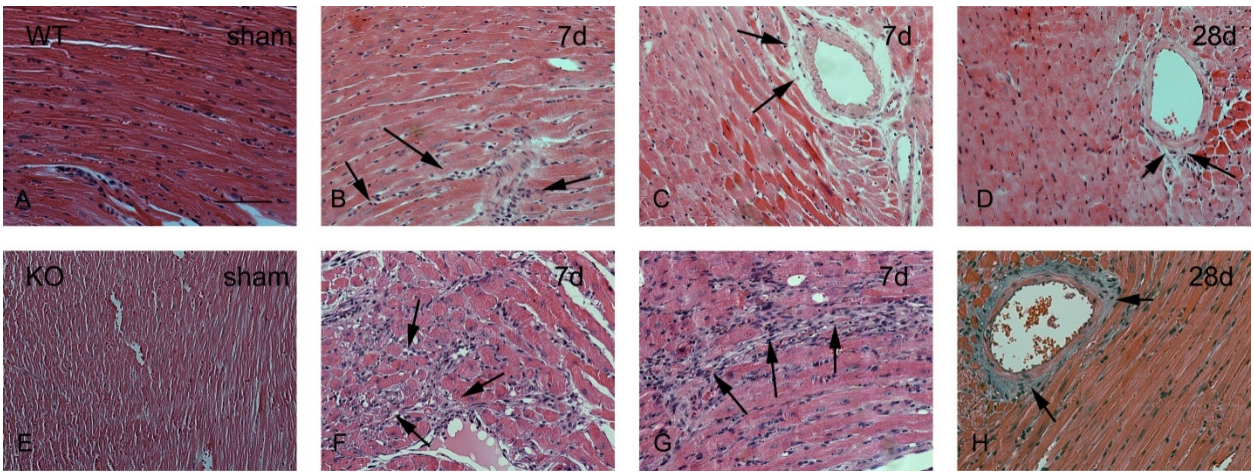

Supplemental figure 7: tTG loss is associated with expansion and increased cellularity of the cardiac interstitium following pressure overload. Hematoxylin/eosin staining of sham and pressure overloaded WT (A-D) and tTG KO (E-H) hearts after 7-28 days of TAC. Pressure overload results in expansion of the cardiac interstitium and development of perivascular fibrosis in both WT and tTG KO animals (arrows). When compared with corresponding WT animals, tTG KOs exhibit accentuated widening of the cardiac interstitium and increased cellularity in interstitial and perivascular areas (scale bar=50μm).

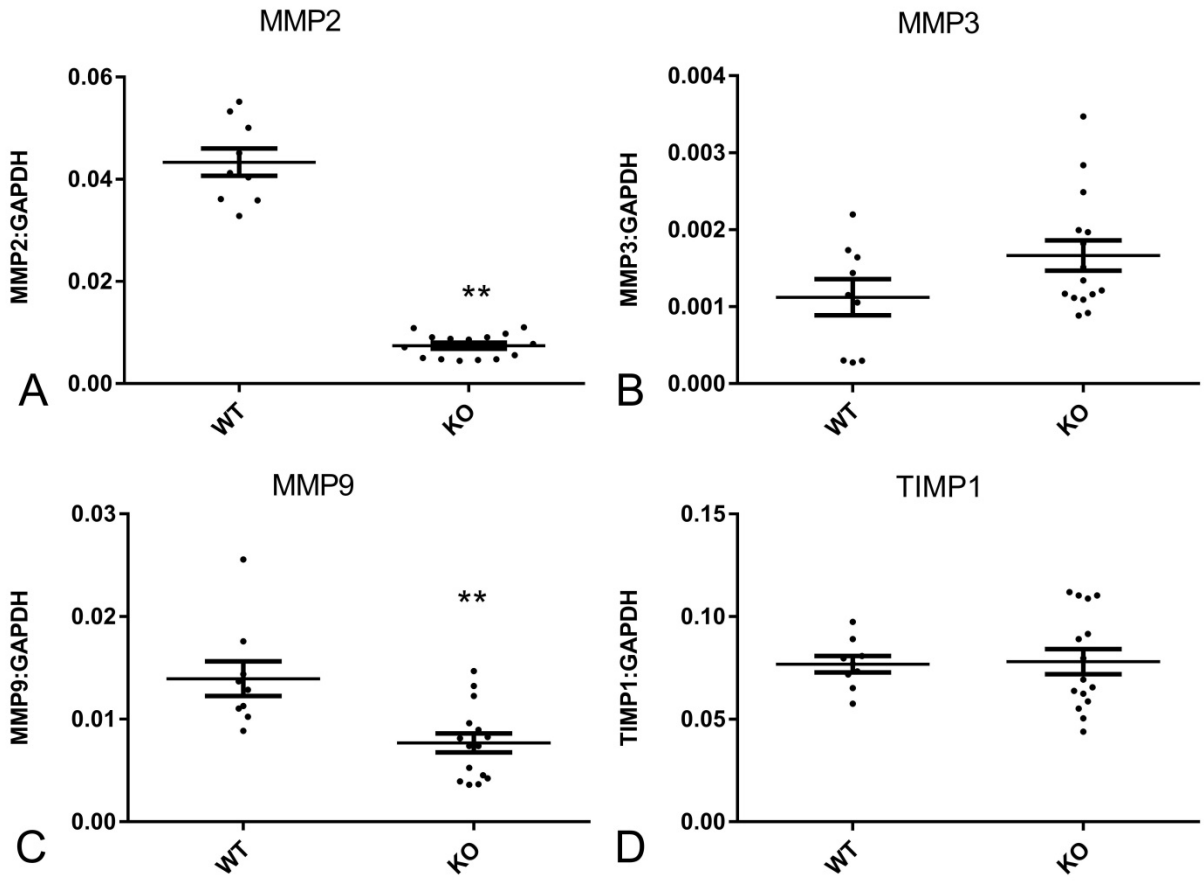

Supplemental figure 8: Increased MMP2 activity in pressure-overloaded tTG KO hearts is not due to accentuated macrophage derived MMP synthesis. CD11b+ myeloid cells were harvested from WT and tTG KO pressure-overloaded hearts to assess expression of MMPs and TIMPs. Myeloid cells harvested from tTG KO animals had markedly lower MMP2 (A) and MMP9 (C) mRNA synthesis. MMP3 (B) and TIMP1 (D) mRNA levels were comparable between WT and KO cells (n=9-15/group, unpaired t-test).

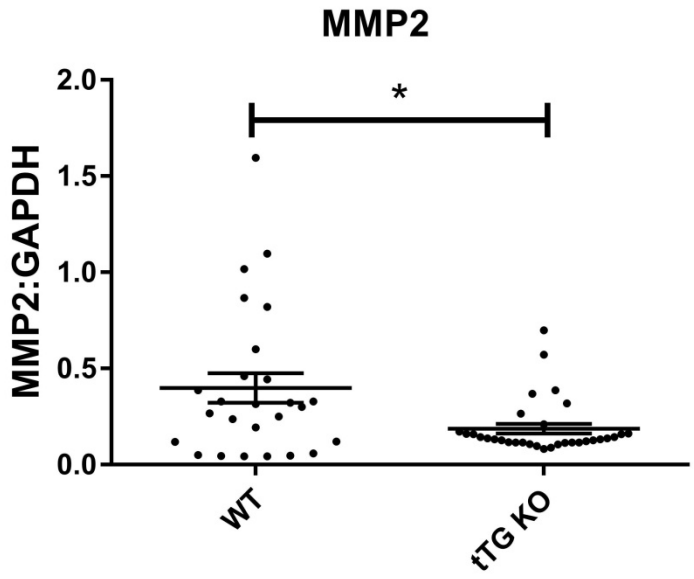

Supplemental figure 9: tTG KO cardiac fibroblasts, cultured in collagen pads exhibit reduced MMP2 mRNA expression when compared to WT cells (*$p<0.05$, n=26/group, Mann-Whitney test).

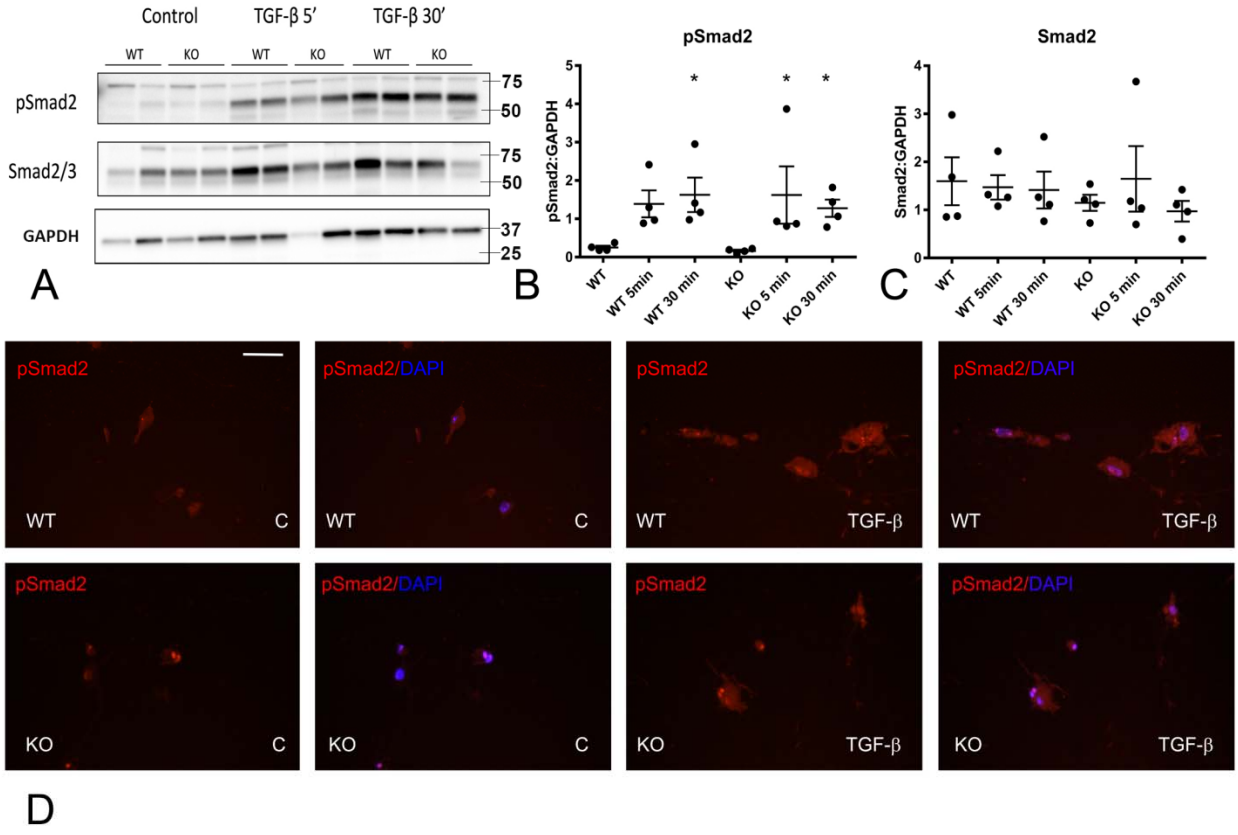

Supplemental figure 10: tTG loss does not affect activation of TGF-β/Smad signaling in cardiac fibroblasts. A-C: Because intracellular tTG may modulate growth factor responses we compared TGF-β/Smad signaling between WT and tTG KO cells using western blotting for phosphorylated Smad2 and Smad2 (A). Quantitative analysis showed that tTG KO and WT cells had comparable activation of Smad2 signaling upon stimulation with TGF-β1 (10ng/ml) (B) (*$p<0.05$ vs. corresponding control, n=4-6, Kruskal-Wallis test). Smad2 expression levels were comparable between groups (C). D. In order to examine the effects of tTG loss on fibroblast Smad2 activation in cells cultured in a matrix environment, we assessed Smad2 phosphorylation in fibroblast-populated collagen pads. Both WT cells (upper row) and tTG KO cells (lower row) showed significantly increased pSmad2 immunoreactivity in the cytoplasm and nucleus after stimulation with TGF-β1 (scalebar=40μm). Images show representative findings from 3 independent experiments.

REFERENCES

1. De Laurenzi V Melino G. Gene disruption of tissue transglutaminase. *Mol Cell Biol* 2001;**21**:148-155.
2. Xia Y, Dobaczewski M, Gonzalez-Quesada C, Chen W, Biernacka A, Li N, Lee DW Frangogiannis NG. Endogenous thrombospondin 1 protects the pressure-overloaded myocardium by modulating fibroblast phenotype and matrix metabolism. *Hypertension* 2011;**58**:902-911.
3. Chen W, Saxena A, Li N, Sun J, Gupta A, Lee DW, Tian Q, Dobaczewski M Frangogiannis NG. Endogenous IRAK-M attenuates postinfarction remodeling through effects on macrophages and fibroblasts. *Arterioscler Thromb Vasc Biol* 2012;**32**:2598-2608.
4. Nagueh SF, Appleton CP, Gillebert TC, Marino PN, Oh JK, Smiseth OA, Waggoner AD, Flachskampf FA, Pellikka PA Evangelista A. Recommendations for the evaluation of left ventricular diastolic function by echocardiography. *J Am Soc Echocardiogr* 2009;**22**:107-133.
5. Hilfiker-Kleiner D, Hilfiker A, Fuchs M, Kaminski K, Schaefer A, Schieffer B, Hillmer A, Schmiedl A, Ding Z, Podewski E, Podewski E, Poli V, Schneider MD, Schulz R, Park JK, Wollert KC Drexler H. Signal transducer and activator of transcription 3 is required for myocardial capillary growth, control of interstitial matrix deposition, and heart protection from ischemic injury. *Circ Res* 2004;**95**:187-195.
6. Biernacka A, Cavalera M, Wang J, Russo I, Shinde A, Kong P, Gonzalez-Quesada C, Rai V, Dobaczewski M, Lee DW, Wang XF Frangogiannis NG. Smad3 Signaling Promotes Fibrosis While Preserving Cardiac and Aortic Geometry in Obese Diabetic Mice. *Circ Heart Fail* 2015;**8**:788-798.
7. Trueblood NA, Xie Z, Communal C, Sam F, Ngoy S, Liaw L, Jenkins AW, Wang J, Sawyer DB, Bing OH, Apstein CS, Colucci WS Singh K. Exaggerated left ventricular dilation and reduced collagen deposition after myocardial infarction in mice lacking osteopontin. *Circ Res* 2001;**88**:1080-1087.
8. Hilfiker-Kleiner D, Kaminski K, Kaminska A, Fuchs M, Klein G, Podewski E, Grote K, Kiian I, Wollert KC, Hilfiker A Drexler H. Regulation of proangiogenic factor CCN1 in cardiac muscle: impact of ischemia, pressure overload, and neurohumoral activation. *Circulation* 2004;**109**:2227-2233.
9. Christia P, Bujak M, Gonzalez-Quesada C, Chen W, Dobaczewski M, Reddy A Frangogiannis NG. Systematic characterization of myocardial inflammation, repair, and remodeling in a mouse model of reperfused myocardial infarction. *J Histochem Cytochem* 2013;**61**:555-570.
10. Zion O, Genin O, Kawada N, Yoshizato K, Roffe S, Nagler A, Iovanna JL, Halevy O Pines M. Inhibition of transforming growth factor beta signaling by halofuginone as a modality for pancreas fibrosis prevention. *Pancreas* 2009;**38**:427-435.
11. Whittaker P, Kloner RA, Boughner DR Pickering JG. Quantitative assessment of myocardial collagen with picrosirius red staining and circularly polarized light. *Basic Res Cardiol* 1994;**89**:397-410.
12. Dobaczewski M, Bujak M, Li N, Gonzalez-Quesada C, Mendoza LH, Wang XF Frangogiannis NG. Smad3 signaling critically regulates fibroblast phenotype and function in healing myocardial infarction. *Circ Res* 2010;**107**:418-428.
13. Mukherjee D Sen S. Collagen phenotypes during development and regression of myocardial hypertrophy in spontaneously hypertensive rats. *Circ Res* 1990;**67**:1474-1480.
14. Saxena A, Chen W, Su Y, Rai V, Uche OU, Li N Frangogiannis NG. IL-1 Induces Proinflammatory Leukocyte Infiltration and Regulates Fibroblast Phenotype in the Infarcted Myocardium. *J Immunol* 2013;**191**:4838-4848.
15. Martinez FO, Helming L, Milde R, Varin A, Melgert BN, Draijer C, Thomas B, Fabbri M, Crawshaw A, Ho LP, Ten Hacken NH, Cobos Jimenez V, Kootstra NA, Hamann J, Greaves DR, Locati M, Mantovani A Gordon S. Genetic programs expressed in resting and IL-4 alternatively activated mouse and human macrophages: similarities and differences. *Blood* 2013;**121**:e57-69.